

# Origins of the Thick Disk as Traced by the Alpha-Elements of Metal-Poor Giant Stars Selected from RAVE

G. R. Ruchti<sup>1</sup>, J. P. Fulbright<sup>1</sup>, R. F. G. Wyse<sup>1</sup>, G. F. Gilmore<sup>2</sup>, O. Bienaymé<sup>3</sup>, J. Binney<sup>4</sup>, J. Bland-Hawthorn<sup>5</sup>, R. Campbell<sup>6</sup>, K. C. Freeman<sup>7</sup>, B. K. Gibson<sup>8</sup>, E. K. Grebel<sup>9</sup>, A. Helmi<sup>10</sup>, U. Munari<sup>11</sup>, J. F. Navarro<sup>12</sup>, Q. A. Parker<sup>13</sup>, W. Reid<sup>13</sup>, G. M. Seabroke<sup>14</sup>, A. Siebert<sup>3</sup>, A. Siviero<sup>12,15</sup>, M. Steinmetz<sup>15</sup>, F. G. Watson<sup>16</sup>, M. Williams<sup>17</sup>, T. Zwitter<sup>17,18</sup>

## ABSTRACT

Theories of thick disk formation can be differentiated by measurements of stellar elemental abundances. We have undertaken a study of metal-poor stars selected from the RAVE spectroscopic survey of bright stars to establish whether or not there is a significant population of metal-poor thick-disk stars ( $[\text{Fe}/\text{H}] \lesssim -1.0$ ) and to measure their elemental abundances. In this paper, we present abundances of four  $\alpha$ -elements (Mg, Si, Ca, Ti) and iron for a subsample of 212 RGB and 31 RC/HB stars from this study. We find that the  $[\alpha/\text{Fe}]$  ratios are enhanced implying that enrichment proceeded by purely core-collapse supernovae. This requires that star formation in each star forming region had a short duration. The relative lack of scatter in the  $[\alpha/\text{Fe}]$  ratios implies good mixing in the ISM prior to star formation. In addition, the ratios resemble that of the halo, indicating that the halo and thick disk share a similar massive star IMF. We conclude that the  $\alpha$ -enhancement of the metal-poor thick disk implies that direct accretion of stars from dwarf galaxies similar to surviving dwarf galaxies today did not play a major role in the formation of the thick disk.

---

<sup>1</sup>Johns Hopkins University, 3400 N Charles Street, Baltimore, MD 21218, USA; gruchti@pha.jhu.edu

<sup>2</sup>Institute of Astronomy, University of Cambridge, Madingley Road, Cambridge CB3 0HA, UK

<sup>3</sup>Observatoire de Strasbourg, 11 Rue de L'Université, 67000 Strasbourg, France

<sup>4</sup>Rudolf Pierls Center for Theoretical Physics, University of Oxford, 1 Keble Road, Oxford OX1 3NP, UK

<sup>5</sup>Sydney Institute for Astronomy, School of Physics A28, University of Sydney, NSW 2006, Australia

<sup>6</sup>Western Kentucky University, 1906 College Heights Blvd., Bowling Green, KY 42101, USA

<sup>7</sup>RSAA Australian National University, Mount Stromlo Observatory, Cotter Road, Weston Creek, Canberra, ACT 2611, Australia

<sup>8</sup>Jeremiah Horrocks Institute for Astrophysics & Super-computing, University of Central Lancashire, Preston, UK

<sup>9</sup>Astronomisches Rechen-Institut, Zentrum für Astronomie der Universität Heidelberg, D-69120 Heidelberg, Germany

<sup>10</sup>Kapteyn Astronomical Institute, University of Groningen, Postbus 800, 9700 AV Groningen, Netherlands

<sup>11</sup>INAF Osservatorio Astronomico di Padova, Via dell'Osservatorio 8, Asiago I-36012, Italy

<sup>12</sup>University of Victoria, P.O. Box 3055, Station CSC, Victoria, BC V8W 3P6, Canada

<sup>13</sup>Macquarie University, Sydney, NSW 2109, Australia

<sup>14</sup>Mullard Space Science Laboratory, University College London, Holmbury St. Mary, Dorking, RH5 6NT, UK

<sup>15</sup>Astrophysikalisches Institut Potsdam, An der Sternwarte 16, D-14482 Potsdam, Germany

<sup>16</sup>Anglo-Australian Observatory, P.O. Box 296, Epping, NSW 1710, Australia

<sup>17</sup>Faculty of Mathematics and Physics, University of Ljubljana, Jadranska 19, Ljubljana, Slovenia

<sup>18</sup>Center of Excellence SPACE-SI, Ljubljana, Slovenia

*Subject headings:* Galaxy: abundances — Galaxy: disk — stars: abundances — stars: late-type

## 1. Introduction

Thick disks are a common and significant stellar component in most disk galaxies, and their formation is an integral part of disk-galaxy formation. Most of the stars in the thick disk of the Milky Way Galaxy are old,  $\gtrsim 10$  Gyr (Gilmore & Wyse 1985; Reddy et al. 2006), and so they can serve as fossil records of the formation processes in early Galactic evolution. An important method for unlocking this information is the analysis of the elemental abundance patterns in thick-disk stars. Of particular importance are the ratios of the  $\alpha$ -elemental (eg. Mg, Si, Ca, Ti) abundances to iron, which provide information about the past star formation and IMF of a stellar population (cf. Wyse 2010). This approach is complementary to comparisons of the age distribution of thick-disk stars with theoretical expectations (e.g. Wyse 2009).

Models of the formation of the thick disk, including scenarios ranging from migration of stars from the inner disk (Schönrich & Binney 2009) to heating of the thin disk due to mergers (e.g. Villalobos & Helmi 2008), make specific predictions about the chemical abundance properties of the metal-weak (and oldest) stellar population in the thick disk. In hierarchical clustering, heating of pre-existing thin stellar disks by merging continues until late times. In this case, an intermediate-age thick disk would emerge from heating of the thin disk, in conflict with the old ages found. A proposed solution is that the old thick disk is a result of direct accretion of old stars from a few satellite galaxies (Abadi et al. 2003). The metal-poor stars in the thick disk would then show the same chemical enrichment as the parent satellite. Depending on the mass, orbit, and density profile of each accreted satellite, the  $\alpha$ -abundance patterns of the thick disk would also vary with Galactic radius. The identification and chemical analysis of metal-poor thick-disk stars beyond the solar neighborhood is therefore very important.

The existence of a significant metal-weak ( $[\text{Fe}/\text{H}] \leq -1.0$ ) thick disk remains controversial. The metal-poor thick disk was identified in both the field (Norris et al. 1985; Morrison et al. 1990; Wyse & Gilmore 1995; Chiba & Beers 2000), and in globular clusters (Dinescu et al. 1999). The apparent lack of blue horizontal-branch and RR Lyrae stars in the thick disk, however, argues against an old metal-poor component (Kinman et al. 2009). The small number of metal-poor thick-disk stars studied to date (Fulbright 2002; Bensby et al. 2003; Brewer & Carney 2006; Reddy et al. 2006; Reddy & Lambert 2008) have high  $[\alpha/\text{Fe}]$  ratios, implying they formed in a short-duration star formation event, and old ages when estimates are available. These samples, however, have been limited to very bright stars within the solar neighborhood.

The unprecedented size of the Radial Velocity Experiment spectroscopic survey (RAVE, Steinmetz et al. 2006) and its selection without either kinematic or metallicity criteria provide a unique opportunity to study a statistically significant sample of bright metal-poor thick-disk stars, as described below. Our sample both probes a much larger volume and extends to lower metallicities than any previous thick-disk sample with elemental abundances. We here present elemental abundance results for a subsample of (predominantly) red giant branch (RGB) and red clump/horizontal branch (RC/HB) stars.

## 2. Observations

### 2.1. Candidate Selection

Candidate metal-poor thick-disk stars were selected from RAVE, a *magnitude-limited* survey that uses the 6dF spectrograph on the UK Schmidt telescope to obtain high S/N,  $\mathcal{R} \sim 7500$  spectra ( $\lambda 8410 \text{ \AA} - \lambda 8795 \text{ \AA}$ ) of stars in the southern sky with  $I < 13$ . The RAVE pipeline provides estimates of radial velocities and stellar parameters (effective temperature,  $T_{\text{eff}}$ ; gravity,  $\log g$ ; metallicity,  $[M/H]$ ) through fits to a grid of synthetic spectra (see Zwitter et al. 2008). The stars are bright enough that they have proper motion measurements in the literature (included in the RAVE database). We selected candidate metal-poor disk stars with  $[M/H] \leq -0.7$  and estimates of 3-D space motions, based on parameter values in the database, consistent with disk kinematics.

### 2.2. High Resolution Echelle Observations

High resolution spectroscopy provides robust abundances for most elements. We obtained data between May 2007 and February 2009 using the following spectrographs/telescopes: MIKE/Magellan-Clay, FEROS/MPG 2.2-m, UCLES/AAT, and ARCES/APO-3.5. All instruments have a resolving power between 35,000-45,000 and a spectral coverage of  $\lambda 3500 \text{ \AA} - \lambda 9500 \text{ \AA}$ , except for UCLES which covers  $\lambda 4460 \text{ \AA} - \lambda 7270 \text{ \AA}$ . The raw FEROS spectra were reduced using the Data Reduction System within ESO-MIDAS, while all other spectra were reduced using the echelle package in IRAF<sup>1</sup>. The final spectra yielded a S/N  $> 100$  per pixel at  $\lambda 5000 \text{ \AA} - \lambda 6000 \text{ \AA}$  and a minimum S/N  $\sim 40$  around  $\lambda 4000 \text{ \AA}$ , sufficient for abundance analysis.

A total of  $\sim 500$  spectra for candidate metal-poor thick-disk stars were obtained. We removed potentially problematic stars (e.g. hot stars, fast rotators), in addition to 4 radial-velocity outliers, probable binary stars, after comparison with RAVE ( $\Delta V > 20 \text{ km s}^{-1}$ ). Ten of the remaining stars have repeat echelle observations. We here report on the subsample of evolved stars ( $\log g < 3.3$ ), consisting of 212 RGB stars and 31 RC/HB stars, for which a uniform analysis is implemented.

## 3. Abundance Analysis

Our initial analysis followed the methodology of Fulbright (2000, hereafter F00). We combined the line lists from F00 and Johnson (2002), thus extending the analysis to extremely metal-poor stars. Equivalent widths (EWs) were measured using the ARES code (Sousa et al. 2007), which fits a Gaussian to each line. Strong lines with  $EW \geq 110 \text{ m\AA}$  were removed to minimize poor fits. Comparisons with hand-measured EWs for 12 metal-poor stars resulted in a mean difference  $EW_{\text{hand}} - EW_{\text{ARES}} \sim -0.1 \pm 3 \text{ m\AA}$ , sufficiently small that line-measurement biases are unimportant.

The MOOG analysis program (Snedden 1973) was utilized in an iterative procedure to compute elemental abundances using 1-D, LTE, plane-parallel Kurucz model atmospheres,<sup>2</sup>. The stellar temperature was set by the excitation temperature method based on Fe I lines. The  $\log g$  value was set by minimizing the difference between the calculated abundance of iron from the Fe I and Fe II lines. A microturbulent velocity was selected

---

<sup>1</sup>Distributed by NOAO, operated by AURA under cooperative agreement with the NSF.

<sup>2</sup><http://kurucz.harvard.edu/>.

to minimize the slope of the relationship between the iron abundance derived from Fe I lines and the value of the reduced width of the line. The metallicity value of the stellar atmosphere was chosen to match the iron abundance in the analysis. The repeat observations gave internal errors of 55 K, 0.1 dex, and 0.06 dex in  $T_{\text{eff}}$ ,  $\log g$ , and  $[\text{Fe}/\text{H}]$ , respectively, consistent with those of F00.

External errors are critical in distance determination. We tested the accuracy of our parameters using echelle data (obtained for another project) of several globular cluster RGB stars ( $\log g < 2$ ) for which the distances and metallicities are reported in the literature. We also reanalyzed a sample (hereafter F00/Hip) of 6 giant stars from F00 which had Hipparcos parallaxes with acceptable errors ( $\sigma_p/p < 0.2$ ; van Leeuwen 2007). We found that with our initial parameter values many globular cluster giants lay above the RGB-tip, contrary to their location in the CMD, implying that our initial  $\log g$  estimate is too low. Further, the interplay between  $\log g$  and  $T_{\text{eff}}$  in our initial analysis implies that our  $T_{\text{eff}}$  estimate would also be suspect. We therefore computed independent estimates of both gravity and temperature to quantify these effects and hence correct them.

The independent estimate of surface gravity for each globular cluster and F00/Hip star was obtained using the equation  $g_{\text{bol}} = 4\pi GM\sigma T_{\text{eff}}^4/L$ . We adopt our initial estimate of  $T_{\text{eff}}$ , a typical RGB star mass of  $0.8 M_{\odot}$ , and estimated the luminosity from the de-reddened 2MASS  $K_S$  with bolometric corrections derived from González Hernández & Bonifacio (2009) and the published distance. We also derived an independent photometric temperature,  $T_{\text{phot}}$ , for each star using the 2MASS color-temperature transformations from González Hernández & Bonifacio (2009). We assumed that the scale provided by  $T_{\text{phot}}$  does not show spurious trends such as apparently introduced by our initial spectroscopic analysis, and thus can be used to correct our  $\log g$  estimates (as achieved below).

Comparisons between our spectroscopic estimates and these derived values revealed offsets in both temperature and gravity. Further, the difference between our spectroscopic  $T_{\text{eff}}$  estimates and  $T_{\text{phot}}$  is correlated with iron abundance such that our estimate is 300 – 400 K cooler for the lowest metallicity stars (note both Johnson 2002 and Aoki et al. 2005 found similar offsets, albeit using different photometric colors in the derivation of  $T_{\text{phot}}$ ). We therefore corrected  $T_{\text{eff}}$  according to this correlation and repeated the analysis to obtain a new (ionization-balanced) gravity estimate,  $\log g_{\text{phot}}$ . Stars with  $\log g_{\text{phot}} \geq 1$  showed no mean offset with  $\log g_{\text{bol}}$  and we therefore adopted  $\log g_{\text{phot}}$  as our final gravity. The difference,  $\log g_{\text{phot}} - \log g_{\text{bol}}$  is however correlated with  $\log g_{\text{phot}}$  for  $\log g_{\text{phot}} < 1$ . For these stars, we adopt a new  $\log g$  estimate from this correlation along with the corrected temperature above to get a final estimate of the iron abundance. The final temperatures and gravities showed scatter with respect to  $T_{\text{phot}}$  and  $\log g_{\text{bol}}$  of 140 K and 0.2 dex, respectively. In the cases when the iron abundance from Fe I and Fe II do not agree, we chose Fe II as our final estimate, since Fe II is both the dominant species and much less sensitive to non-LTE effects than Fe I (Thévenin & Idiart 1999; Asplund et al. 1999). The iron abundances derived for any given globular cluster showed a star-to-star scatter of  $\pm 0.1$  dex, consistent with our earlier estimates of our internal errors.

We used the above procedure to insure that the derived parameter values for our RAVE sample provide accurate distances.

## 4. Sample Analysis

### 4.1. Distances

Distances are critical and a full description of our technique is given in Ruchti et al. (2010, in prep). In short, distances to our stars are estimated from the most probable  $M_{K_s}$  magnitude in a grid of Padova isochrones (Marigo et al. 2008; Girardi et al. 2002). The temperature, gravity, and metallicity, following the procedure in §3, and their associated errors (as described above) of 140 K, 0.2 dex, and 0.1 dex in  $T_{\text{eff}}$ ,  $\log g$ , and  $[\text{Fe}/\text{H}]$ , respectively, are used in the multi-parameter fit. For the RGB stars, our technique weights each point by the luminosity function, derived from the BaSTI luminosity function tracks (these isolate the RGB from the AGB; Pietrinferni et al. 2004), to emphasize evolutionary stages with longer lifetimes. Several of our stars have  $T_{\text{eff}}$  and  $\log g$  inconsistent with the RGB, and appear to be RC/HB stars. The position of a star on the horizontal branch depends on the mass-loss on the RGB, which is not well understood or modeled. The Padova isochrones, which we use, represent the zero-age HB as one point. Stars within  $2\sigma_{T_{\text{eff}}}$  of this point were assumed to have an absolute magnitude equal to that of that point. Note that  $M_{K_s}$  ranges between only 0.1 – 0.2 magnitudes during the slow-evolution phase of core-helium burning. We assumed an old age for the RGB stars, performing a weighted average over isochrones of ages 10, 11, and 12 Gyr (reducing the age to 5 Gyr increased the distances by only 10%), while we assume an age of 12 Gyr for the RC/HB stars.

We first applied this technique to the cluster and F00/Hip stars. Our distances differed from literature values by only  $-2 \pm 15\%$  for the cluster stars and  $-4 \pm 13\%$  for the F00/Hip stars. We therefore adopted a conservative estimate of 20% error on the distance, including both scatter and offset. Distance estimates based on RAVE pipeline values of stellar parameters are now available (Breddels et al. 2010; Zwitter et al. 2010). Our distance estimates for the 172 stars with  $|\log g_{\text{echelle}} - \log g_{\text{RAVE}}| < 0.5$  are shorter than those of Zwitter et al. by  $15 \pm 24\%$ . Note that our technique was optimized for metal-poor stars with echelle parameters, while Zwitter et al. (2010) optimized their method for all stars in the RAVE catalog, which have a high mean metallicity and typically younger ages.

The average distance to our RAVE stars is  $\sim 2$  kpc; all within  $\sim 7$  kpc, except one at  $\sim 16$  kpc. The majority of our stars have Galactic longitudes between  $\ell = 200^\circ$  and  $50^\circ$  and Galactic latitudes  $|b| > 25^\circ$ , extending to an average vertical height of  $|z| \gtrsim 1$  kpc.

### 4.2. Population Assignments

The 3-D, cylindrical space motion ( $V_{\text{H}}$ ,  $V_{\text{Θ}}$ ,  $V_{\text{Z}}$ ) of each star was computed by combining the derived distances and radial velocities with proper motions from the RAVE database. We adopted (10, 5.25, 7.17)  $\text{km s}^{-1}$  (Dehnen & Binney 1998) for the solar motion<sup>3</sup> and  $V_{\text{LSR}} = 220 \text{ km s}^{-1}$ . Each component of a star’s space motion was then re-sampled 10,000 times, assuming a normal distribution centered on our estimate of the component velocity, with standard deviation equal to the propagated error in the velocity. We computed the probability that each re-sampled value of the space motion was drawn from a given kinematic population, based on the combined local characteristic Gaussian distributions assumed for each Galactic

---

<sup>3</sup>Our assignment method is insensitive to values within the range of recent estimates (e.g. Schönrich et al. 2010).

population (see Table 1), defined as:

$$P(V_{\Pi}, V_{\Theta}, V_Z) \propto \exp \left( -\frac{V_{\Pi}^2}{2\sigma_{\Pi}^2} - \frac{(V_{\Theta} - 220 - \langle V_{\Theta} \rangle)^2}{2\sigma_{\Theta}^2} - \frac{V_Z^2}{2\sigma_Z^2} \right), \quad (1)$$

where, for each population,  $\sigma_{\Pi}$ ,  $\sigma_{\Theta}$ , and  $\sigma_Z$  are the characteristic velocity dispersions and  $\langle V_{\Theta} \rangle$  is the mean rotational velocity (corrected for the Sun’s motion). Note that Gaussian distributions are a first-order approximation, and the distribution functions may be much more complex (cf., Binney 2010). We did not include vertical gradients in kinematics or metallicity-kinematical relations at this point.

Table 1: Local Characteristic Velocity Distributions.

	$\sigma_{\Pi}$ (km s <sup>-1</sup> )	$\sigma_{\Theta}$ (km s <sup>-1</sup> )	$\sigma_Z$ (km s <sup>-1</sup> )	$\langle V_{\Theta} \rangle$ (km s <sup>-1</sup> )	Ref.
Thin Disk	39	20	20	-15	Soubiran et al. (2003)
Thick Disk	63	39	39	-51	Soubiran et al. (2003)
Halo	141	106	94	-220	Chiba & Beers (2000)

For each of the 10,000 samplings of the space motion of a given star, an assignment to the thick disk was made if that probability was 4 times that of either the thin disk or halo, with an analogous procedure for thin disk and halo. Intermediate populations, thin/thick and thick/halo, were assigned for lower values of probability ratios. A star was assigned to the Galactic population with the highest number of occurrences from the 10,000 re-sampled points.

A second population assignment was determined by comparing a star’s position in the Galaxy to the characteristic density distributions of each Galactic component (from Jurić et al. 2008), following the same Monte Carlo procedure as the space motion criterion. This criterion works well far from the Galactic plane, however discrimination is difficult close to the plane since a star must have  $|z| = 2$  kpc before the thick disk probability is 4 times that of the thin disk. The assignment is therefore restricted to choosing only halo over thick disk or thick over thin disk.

The final population assignment was then the result from the space motion criterion, unless overridden by the boundary condition set from the star’s position. Our results are consistent with each star’s position in the reduced proper motion diagram. These final assignments were 73 thick disk, 1 thin disk, 22 thick/thin, 31 thick/halo, and 116 halo. The Toomre diagram (Figure 1) illustrates the correspondence between these population assignments and velocities. It is not surprising that many candidates were assigned to the halo since, with our final parameter values, our sample extends to large distances and high velocities.

## 5. Alpha Element Abundance Results

Elemental abundances were derived through MOOG after all stellar parameter corrections in §3. Figure 2 displays  $[\alpha/\text{Fe}]$  as a function of  $[\text{Fe}/\text{H}]$  for several  $\alpha$ -elements. Note that the range of  $[\text{Fe}/\text{H}]$  shows that our selection function from RAVE was efficient. The main bulk of thick-disk stars extend to  $[\text{Fe}/\text{H}] \sim -1.8$ , with 5 additional stars assigned to the thick disk below -2 dex. Further, these stars have  $[\alpha/\text{Fe}]$  significantly above solar, with relatively low scatter, and blend smoothly into the halo stars.

The kinematics of the metal-poor thick disk may differ from the canonical thick disk (Carollo et al. 2010), with higher velocity dispersions and a slower rotational velocity. Adopting  $\langle V_{\Theta} \rangle = -100$  km s<sup>-1</sup> (see

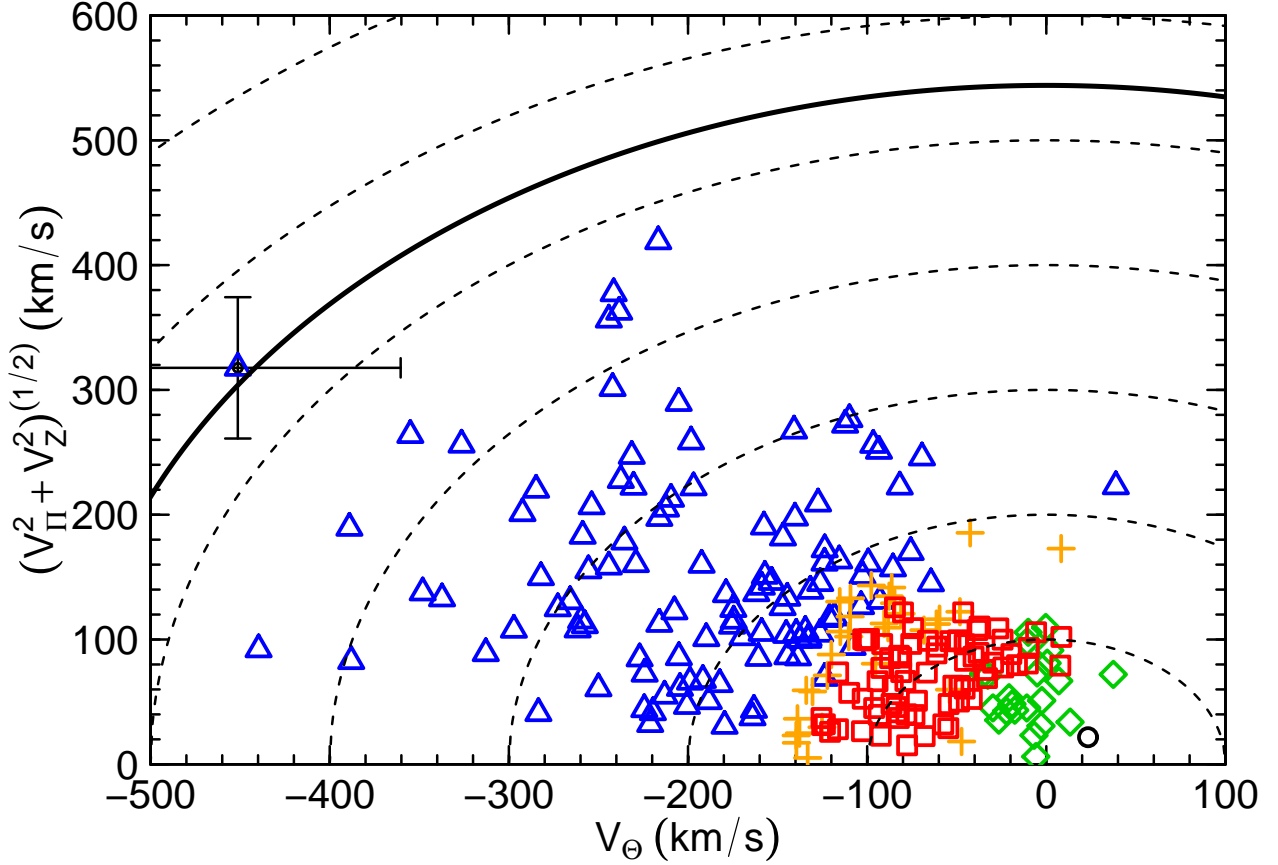


Fig. 1.— The Toomre Diagram for our sample with  $\sigma_{V_\Theta} < 100 \text{ km s}^{-1}$ . The black circle, green diamonds, red squares, orange plus signs, and blue triangles correspond to thin disk, thin/thick, thick disk, thick/halo, and halo stars, respectively. The dashed curves indicate constant space motion, in steps of  $100 \text{ km s}^{-1}$ . The thick solid curve is an estimate of the local escape velocity (Smith et al. 2007). The total velocity error depends on distance and proper motion errors, with the typical  $1\sigma$  error  $< 20 \text{ km s}^{-1}$ . The star near the estimated escape velocity is the subject of a future paper.

Gilmore et al. 2002), would reassign several stars with thick/halo population assignments to the thick disk. There would be no change in our conclusions, since these stars have similar  $\alpha$ -enhancement to the metal-poor thick disk and halo.

A two-component halo at  $[\text{Fe}/\text{H}] \gtrsim -1$ , separated in  $[\text{Mg}/\text{Fe}]$  enhancement, has been reported by Nissen & Schuster (2010). Indeed, several of our halo stars in this metallicity range have values of  $[\text{Mg}/\text{Fe}] \lesssim 0.2$ , but other  $\alpha$ -elements show little spread, in contrast to Nissen & Schuster (2010). We will return to this in another paper.

## 6. Discussion

We have computed the abundances of four major  $\alpha$ -elements for RGB and RC/HB stars in our sample, with  $-0.5 \gtrsim [\text{Fe}/\text{H}] \gtrsim -2.8$ . About 40% of these stars have the highest probability of being (thick or thin)

disk stars and probe distances much further than any earlier investigation. Previous high-resolution samples (e.g. Reddy & Lambert 2008) did identify metal-poor thick disk stars with  $[\text{Fe}/\text{H}] < -1.5$ . We have increased this number by almost an order of magnitude, finding 24 thick disk stars with  $[\text{Fe}/\text{H}] < -1.5$  that extend to metallicities below -2 dex. The  $[\alpha/\text{Fe}]$  ratios for these stars are enhanced, indicating that the metal-poor thick disk was enriched by SNe II, before SNe Ia enrichment, implying a timescale for star formation shorter than  $\sim 1$  Gyr. The relatively low scatter in  $[\alpha/\text{Fe}]$  ratios also implies that the ISM was well mixed prior to star formation, and the metal-poor thick-disk stars were enriched by supernovae from an invariant massive star IMF. Further, the metal-poor thick disk and halo stars show similar  $\alpha$ -enhancement, evidence that they were pre-enriched by the same massive star IMF.

The  $\alpha$ -enhancement in the metal-poor thick disk contrasts with that seen in stars of similar metallicities in local dwarf galaxies (as reviewed by Tolstoy et al. 2009). All local dwarf galaxies began star formation early, 10 – 12 Gyr ago, and had extended star formation, often with dominant intermediate-age populations (e.g. Tolstoy et al. 2009). Direct accretion of stars by assimilation of dwarf satellite galaxies into the thin and thick disks in the Abadi et al. (2003) models lasts until  $z \sim 0.7$  ( $\sim 6$  Gyr ago). If the accreted dwarf galaxies formed stars until accretion or had extended star formation similar to surviving dwarfs, then many of the accreted stars will have formed from gas which had significant iron contribution from SNe Ia. Consequently, stars accreted from dwarfs into the thick disk after this time will have low  $[\alpha/\text{Fe}]$  ratios (Unavane et al. 1996), contrary to the enhancement we see in our sample. We conclude that direct accretion of stars from dwarf galaxies similar to surviving dwarf galaxies today did not play a major role in the formation of the thick disk.

Another possibility is that the thick disk was formed from multiple gas-rich minor mergers, as simulated by Brook et al. (2005). This model predicts a high star formation rate from the gas dissipation, consistent with our enhanced  $[\alpha/\text{Fe}]$ , but the model includes direct accretion of stars from the satellite galaxies. We would therefore still expect to find some low  $[\alpha/\text{Fe}]$  stars in the thick disk from *late* merging, which conflicts with our low scatter in the abundance ratios of the metal-poor thick disk. Early heating of a thin stellar disk by mergers, however, is still viable.

The amplitude of radial and vertical gradients in abundances and metallicity will provide diagnostics to further discriminate models of the formation of the thick disk. Our sample, which probes distances much further from the solar neighborhood, is the first for which this can be done, and will be investigated in our next paper (Ruchti et al. 2010, in prep).

GRR, JPF, and RFW acknowledge support through grants from the W. M. Keck Foundation and the Gordon and Betty Moore Foundation, to establish a program of data-intensive science at the Johns Hopkins University, as well as from the NSF (AST-0908326). This publication makes use of data products of the 2MASS survey, a joint project of the University of Massachusetts and IPAC/Caltech, funded by NASA and the NSF. Funding for RAVE ([www.rave-survey.org](http://www.rave-survey.org)) has been provided by institutions of the RAVE participants and by their national funding agencies.

*Facilities:* ARC (*echelle spectrograph*), AAT (*UCLES*), Magellan:Clay (*MIKE*), Max (*FEROS*), UKST (*6dF spectrograph*)

## REFERENCES

Abadi, M. G., Navarro, J. F., Steinmetz, M. & Eke, V. R. 2003, ApJ, 597, 21



- Aoki, W., et al. 2005, *ApJ*, 632, 611
- Asplund, M., Nordlund, Å., Trampedach, R., & Stein, R. F. 1999, *A&A*, 346, L17
- Bensby, T., Feltzing, S. & Lundstrom, I. 2003, *A&A*, 410, 527
- Binney, J. 2010, *MNRAS*, 401, 2318
- Breddels, M. A., et al. 2010, *A&A*, 511, A90
- Brewer, M.-M. & Carney, B. W. 2006, *AJ*, 131, 431
- Brook, C. B., Gibson, B. K., Martel, H. & Kawata, D. 2005, *ApJ*, 630, 298
- Dehnen, W., & Binney, J. J. 1998, *MNRAS*, 298, 387
- Dinescu, D. I., Girard, T. M. & van Altena, W. F. 1999, *AJ*, 117, 1792
- Carollo, D., et al. 2010, *ApJ*, 712, 692
- Chiba, M. & Beers, T. C. 2000, *AJ*, 119, 2843
- Fulbright, J. P. 2000, *AJ*, 120, 1841 (F00)
- Fulbright, J. P. 2002, *AJ*, 123, 404
- Genzel, R. et al. 2006, *Nature*, 442, 786
- Gilmore, G., & Wyse, R. F. G. 1985, *AJ*, 90, 2015
- Gilmore, G., Wyse, R. F. G. & Norris, J. E. 2002, *ApJ*, 574, 39
- Girardi, L. et al. 2002, *A&A*, 391, 195
- González Hernández, J. I., & Bonifacio, P. 2009, *A&A*, 497, 497
- Johnson, J. A. 2002, *ApJS*, 139, 219
- Jurić, M., et al. 2008, *ApJ*, 673, 864
- Kinman, T. D., Morrison, H. L., & Brown, W. R., 2009, *AJ*, 137, 3198
- Kraft, R. P., & Ivans, I. I. 2003, *PASP*, 115, 143
- Marigo, P. et al. 2008, *A&A*, 482, 883
- Morrison, H. L., Flynn, C. & Freeman, K. C. 1990, *AJ*, 100, 1191
- Nissen, P. E., & Schuster, W. J. 2010, *A&A*, 511, L10
- Norris, J., Bessell, M. S. & Pickles, A. J. 1985, *ApJS*, 58, 463
- Pietrinferni, A., Cassisi, S., Salaris, M., & Castelli, F. 2004, *ApJ*, 612, 168
- Reddy, B. E., Lambert, D. L. & Allende Prieto, C. 2006, *MNRAS*, 367, 1329
- Reddy, B. E., & Lambert, D. L. 2008, *MNRAS*, 391, 95

- Schönrich, R., & Binney, J. 2009, MNRAS, 396, 203
- Schönrich, R., Binney, J., & Dehnen, W. 2010, MNRAS, 403, 1829
- Smith, M. et al. 2007, MNRAS, 379, 755
- Snedden, C. 1973, ApJ, 184, 839
- Soubiran, C., Bienaymé, O. & Siebert, A. 2003, A&A, 398, 141
- Sousa, S. G., Santos, N. C., Israelian, G., Mayor, M. & Monteiro, M. J. P. F. G. 2007, A&A, 469, 783
- Steinmetz, M. et al. 2006, AJ, 132, 1645
- Thévenin, F., & Idiart, T. P. 1999, ApJ, 521, 753
- Tolstoy, E., Hill, V., Tosi, M. 2009, ARA&A, 47, 371
- Unavane, M., Wyse, R. F. G., & Gilmore, G. 1996, MNRAS, 278, 727
- van Leeuwen, F. 2007, A&A, 474, 653
- Villalobos, Á., & Helmi, A. 2008, MNRAS, 391, 1806
- Wyse, R. F. G., & Gilmore, G. 1995, AJ, 110, 2771
- Wyse, R. F. G. 2009, IAU Symposium, 254, 501
- Wyse, R. F. G. 2010, IAU Symposium, 265, 461
- Zwitter, T., et al. 2008, AJ, 136, 421
- Zwitter, T., et al. 2010, A&A, accepted, arXiv:1007.4411

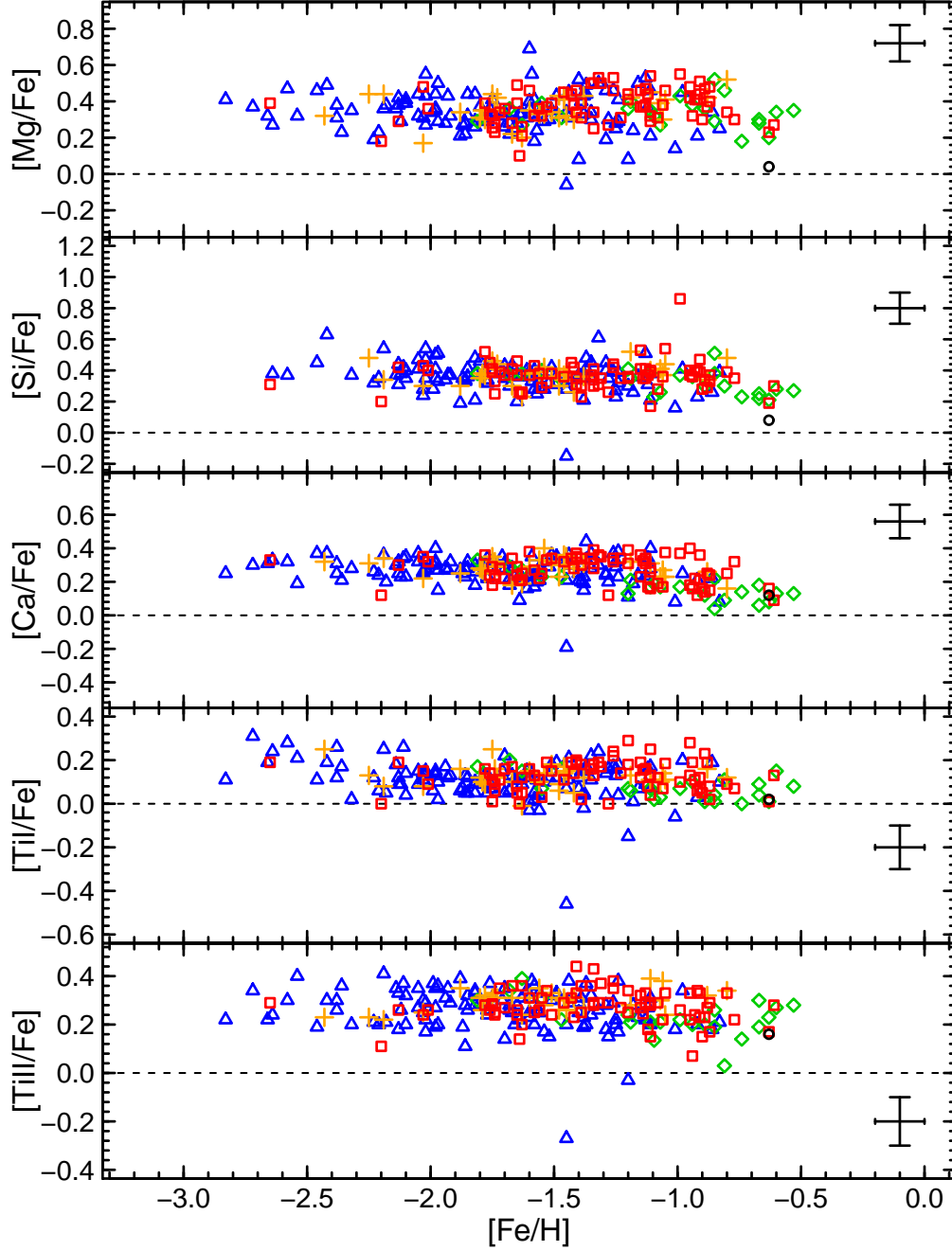


Fig. 2.— Computed  $[\alpha/\text{Fe}]$  ratios versus  $[\text{Fe}/\text{H}]$  for our sample of stars. While Fe II is used to estimate  $[\text{Fe}/\text{H}]$ , element ratios are computed using the iron abundance of the same ionization state as the  $\alpha$ -element (e.g.  $[\text{Si}/\text{Fe}] = [\text{Si I}/\text{Fe I}]$ ) as is suggested by Kraft & Ivans (2003). Color and symbols are the same as in Fig. 1. The cause of the offset between  $[\text{Ti I}/\text{Fe}]$  and  $[\text{Ti II}/\text{Fe}]$  is unclear, but the thick disk and halo still show similar enhancement in each. Two stars of note are the halo star at  $[\text{Fe}/\text{H}] \sim -1.45$  with very low  $\alpha$ -enhancement and the thick disk star at  $[\text{Fe}/\text{H}] \sim -1$  with a very high  $[\text{Si}/\text{Fe}]$  ratio, each of which is the subject of future papers.